EFFECTS OF SUPERCRITICAL CARBONATION CURING ON EXTRUDED VEGETABLE FIBRE-CEMENT

S. F. SANTOS[1], R. SCHMIDT[1], A.E.F.S. ALMEIDA[1], G. H. D. TONOLI[2], H. SAVASTANO JR[1]

[1] *University of São Paulo (USP): Av. Duque de Caxias Norte, 225, CEP 13635-900, Pirassununga, SP, Brazil*

[2] *Federal University of Lavras P. O. Box 3037, CEP 37200-000, Lavras, MG, Brazil*

ABSTRACT

The objective of this work was to investigate the effects of the supercritical carbonation, after pre-curing of three days, on extruded fibre-cement reinforced with bleached eucalyptus pulp and residual sisal fibres. The physical characteristics and mechanical performance was evaluated before and after the soak and dry accelerated ageing cycles test in order to partially simulate the natural weathering mechanism. The supercritical carbonation curing in the initial age led to lower water absorption in the composites and, consequently, to higher bulk density, which improved the microstructure by sealing the opened pores around vegetable fibres. It was observed that the supercritical carbonation curing has a significant effect on crack growth resistance (K_{Ic}) of the extruded fibre-cement. After accelerated ageing of 200 cycles of soaking and drying, the average values of energy of fracture ($\square_{WoF}$) of the carbonated and non-carbonated composites decrease approximately 28% and 56%, respectively.

KEYWORDS:

Sisal fibre, eucalyptus pulp, energy of fracture, fracture toughness.

INTRODUCTION

The vegetable fibre and cellulosic pulp derived from renewable resources, which are widely available in most developing countries, can be used as appropriate materials for cementitious matrix reinforcement. However, significant losses in mechanical performance in long term have been observed in vegetable fibre-cement composites after natural or accelerated ageing (e. g. wet/dry cycling), due to the degradation mechanisms of cellulose fibres in the cementitious environment (Mohr et al., 2007; Tonoli et al., 2009).

As strategy to mitigate long term degradation issues, part of the fibre-cement industry in the world produces fibre-cement composed of Portland cement, finely ground crystalline silica, and cellulose fibre which are autoclaved to ensure appropriate strength, durability and dimensional stability of the composites. The autoclave is steam vented to remove air, then held at 180 ^{o}C for some hours to give a mild cure, a moderate cure or a severe cure (Morton et al., 2006). However, this autoclave curing has exceedingly high energy demands.

Accelerated carbonation can be an alternative route to partially solve long term durability issues of cellulosic fibre-cement. The interaction between carbon dioxide and Portland cement at atmospheric pressure and temperature conditions is a relatively well-known phenomenon. The carbonation effect in the cement paste's chemical composition, porosity and permeability has been widely reported in the literature (Peter et al., 2008; Fabbri et al., 2009). Accelerated carbonation curing has been identified as a technology which may have potential for the mitigation strategy to reduce deterioration of cellulosic fibres and improve mechanical behaviour of these composites (Tolêdo Filho et al., 2003; Almeida et al., 2011; Soroushian et al., 2012). Moreover, Shao and collaborators (2011) suggested the possibility of using an energy efficient carbon dioxide curing to replace autoclaving in cellulose fibre reinforced cement composites production. According to these

researchers, carbonation curing can save considerable amount of energy even with non-integrated technology (Shao et al., 2011).

The use of supercritical CO_2 is an interesting approach for the application of accelerated carbonation curing in cellulosic fibre-cement in the curing stage. The supercritical CO_2 has a high diffusion coefficient due to low viscosity, low surface tension and a density which is about over two orders of magnitude higher than gaseous CO_2 at atmospheric pressure and temperature conditions, factors by which the complete wetting of the complex pores typical for fibre-cement matrices is possible. Thus, the carbonation reactions in cementitious materials in the curing stage can be strongly accelerated by using supercritical CO_2 (Ginneken et al., 2004, García-González et al., 2008).

The objective of this work was to evaluate the effects of the supercritical carbonation in the curing stage, after pre-curing of three days, on physical characteristics and mechanical performance of extruded fibre-cement, reinforced with bleached eucalyptus pulp and residual sisal fibres, before and after the soak and dry accelerated ageing cycles test in order to analyse the long term durability issue.

MATERIALS AND METHODS

The particle size distributions of the ordinary Portland cement (OPC) and ground limestone filler show that 50% of the particles (D_{50}) are finer than 11.8 µm and 14.5 µm, respectively. The quantitative chemical analysis was carried out by X-ray fluorescence equipment PANalytical Axios Advanced. The oxide compositions are listed in Table 1. The loss on ignition is related with the quantity of CO_2 in the raw materials.

Table 1 – X ray fluorescence chemical analysis of the particulate raw material (% by mass).

Oxides	Ordinary Portland cement CPV-ARI	Limestone filler
SiO_2	19.40	9.04
Al_2O_3	4.11	2.16
Fe_2O_3	2.30	1.25
MnO	----	< 0.10
MgO	3.13	8.90
CaO	63.50	39.10
Na_2O	0.24	0.15
K_2O	1.09	0.41
TiO_2	----	0.15
P_2O_5	----	0.16
SO_3	2.97	----
Loss on ignition (1000°C)	3.26	38.58

The mix design was inspired by the formulations for air cured sheets produced by the Hatschek method (changing polymer for sisal fibre) and it is listed in the Table 2. Brazilian ordinary Portland cement type CPV-ARI, correspondent to ASTM-C150, Type I, was chosen because of its finer particle size and higher reactivity in comparison to other blended cements available in the Brazilian market. Additionally, the CPV-ARI type of cement contains higher levels of tricalcium silicate (C_3S) and dicalcium silicate (C_2S) for the formation of C-S-H. The water soluble polymers, hydroxypropyl methylcellulose (HRWR), with 86,000 average molecular weight and 5.39 cP viscosity (at 2% concentration in water at 20°C), provided by Aditex and high range water reducer polyether carboxylic commercially named ADVA 190 provided by Grace, were used as rheological modifiers to promote pseudo-plastic behaviour of the composite. Each additive was applied in the proportion representing 1% of the total mass of the particulate raw materials, and was required to enable the extrusion process. The sisal fibres used in this work are residues of the baler twine industry, donated by the Association for the Sustainable Development of the Sisal Producing Region (APAEB - Valente), Bahia state, Brazil, which were tested as received without any prior conditioning or treatment. The residual sisal fibres, from the cordage production, present a broad and irregular size variation. Therefore, they were cut in order to ensure a narrower

length distribution. After cutting, the fibre length distribution was situated in the range between 2 and 12 mm and whereas the fibre diameter varied between 100 and 350 μm.

Table 2 – Mix design of the cellulosic fibre-cement composites.

Raw material	Content (% by mass)
Ordinary Portland cement (CPV-ARI)	53
Limestone filler	42
Unrefined bleached eucalyptus pulp*	3
Sisal fibres	2

*Fibria S/A

The mixture was homogenized in a mechanical Amadio planetary mixer (capacity of 20 L) during 5 min at 125 rpm, 5 min at medium speed (220 rpm) and finally 5 min at high speed (450 rpm). The water-cement (w/c) ratio was 0.41. The mixture was transferred to a Gelenski MVIG-05 laboratory extruder. The speed of the extruder was approximately 4 mm/s and cross section die width/height ratio was 3.3. The composite was re-circulated into the extruder for 5 min before tailoring the samples. Samples of 15 mm x 50 mm x 200 mm were extruded and put on the steel plates.

Two different curing procedures were applied. The non-carbonated specimens (NC) were cured at 25 °C and 90% RH for two days. Subsequently, the specimens were placed in a water vapour saturated environment (in sealed plastic bags) and maintained in a chamber at 60 ^{o}C for five days (thermal curing). The specimens submitted to carbonation (SC) were initially cured under 25 °C and 90% RH for three days. After that, they were subjected to the experimental supercritical CO_2 treatment. The schematic drawing of the apparatus is shown in Figure 1. The specimens were placed into the chamber with total saturation (99.5% concentration) of supercritical CO_2 at 20 MPa. The CO_2 employed in the experiments was supplied by the White Martins Gases Industriais Company (Brazil). The chamber was immersed in the water bath at 45 °C. The equilibrium treatment conditions were reached after 1 h. The specimens were kept under treatment for 60 min after the achievement of the equilibrium treatment conditions. Subsequently, the specimens were withdrawn from chamber of the apparatus for the treatment with supercritical CO_2, placed in sealed bags and placed in a chamber at 60 °C for four days (thermal curing).
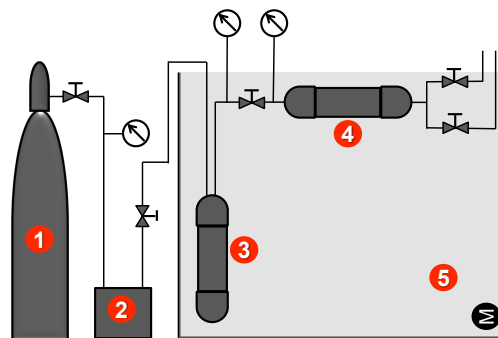
Figure 1 - Schematic drawing of the supercritical CO_2 apparatus. (1) supply tank of CO_2; (2) high pressure pump; (3) lung tank of supercritical CO_2; (4) chamber (5) water bath controlled by a heater (Adapted from Martinez-Correa et al., 2011).

The accelerated ageing test method aims to partially simulate the natural ageing with exposure to soaking and drying cycles. Specimens were successively immersed into water at 20 ± 5°C for 170 min and, after an interval of 10 min they were heated to the temperature of 70 ± 5°C for 170 min in a ventilated oven. Another interval of 10 min at room temperature elapses before the subsequent cycle, as recommended by EN 494 Standard (1994). A total of 200 cycles was executed in order to better identify the modification in the physical and mechanical behavior of the composites.

Mechanical tests in equilibrium with the temperature and air humidity of the laboratory were performed, 20 days after curing, applying a servo-hydraulic mechanical testing machine MTS model 370.02 controlled by MultiPurpose TestWare System. Prismatic specimens were prepared using a diamond saw blade, prior to

grinding and final polishing of the specimen sides and having nominal dimensions of 12 mm x 16 mm x 80 mm. The three-point bending test configuration with span of 64 mm was used. Eight specimens were used for each mechanical test: modulus of rupture, fracture toughness and energy of fracture.

Modulus of rupture values (MOR) were obtained using cross-head speed of 5 mm/min.

Fracture toughness, K_{Ic}, that evaluates the initial crack growth resistance, was determined using the single-edge notch bend SENB-type specimens, with the same dimensions and finishing mentioned above. The prismatic specimens were prepared, with a centred flat notch with depth equal to 10% of specimen height and notch tip profile in the shape of a "V" with angle of about 30° using a diamond disc of 0.5 mm thick to simulate a sharp crack in order to establish the critical defect size and catastrophic fracture. A cross-head speed of 15 mm/min was applied. The calculation of the value of K_{Ic} was done according to Sakai and Bradt (1993).

The fracture energy test was performed with the SENB-type specimen. The specimens with a centred flat notch with 30% of specimen height and notch tip in "V" with angle of about 30° were prepared using diamond disc of 0.5 mm thick. A cross-head speed of 10 µm/min was adopted and controlled by the actuator displacement to guarantee stable growth of the crack (Nakayama, 1965).

The work done by the machine to completely propagate the crack along the specimen divided by two times the projected area of the fracture surface (cross-section of the specimen) was used to obtain the fracture energy, $\square_{WoF}$. The integration of the force-displacement curve was made up to the point where the force decreased to 5% of its maximum value reached during the test. Additionally, a fracture mechanics parameter was obtained to analyse the fracture process from the load-displacement curves and the fracture energy tests called "relative work of crack-propagation" (Kajita et al., 1997; Ribeiro and Rodrigues, 2010). This fracture mechanics parameter is obtained by dividing the work of crack propagation by the elastic work. The elastic work is that one performed from the zero load up to the point of the maximum load. Although up to this point some crack propagation could already occur, that indicates the beginning of the growth of the crack, starting from the tip of the notch. Therefore the area under force-displacement curve can be divided into two distinct regions: a region characterized by a linear elastic behaviour, with increasing load until a critical size is reached at the highest load point of the curve and a remainder region that is characterized by continuous and stable propagation of the crack as the load decreases. This ratio considers all the work made for the effective crack propagation in relation to the elastic and plastic energy stored into the system. Therefore, the higher this relative work means a more resistant the material against the propagation of the crack (Ribeiro and Rodrigues, 2010).

The hydration process of Portland cement can also be evaluated by measuring the mass loss of hydrated samples up to 800 °C. The thermogravimetric analyses (TGA) were performed using TGA 2050 Thermogravimetric Analyzer V5.1A equipment. The experimental conditions were: N_2 gas dynamic atmosphere (40 mL/min); heating rate (10 °C/min); platinum top-opened crucible. The samples were heated in the range of 20–900 °C at a constant rate. The amount of Calcium Hydroxide, $Ca(OH)_2$, and Calcium Carbonate, $CaCO_3$, was estimated from the weight loss measured in the TGA curve between the initial and final temperature of the corresponding DTG peak.

The physical properties, bulk density (BD) and water absorption (WA) were obtained following procedures specified by the ASTM C 948 Standard (1981). Mercury intrusion porosimetry (MIP) measurements have been carried out to determine the pore size distribution of the composites using the Micromeritics Poresizer 9320 mercury porosimeter, assuming a contact angle of 130° and the value of surface tension of 0.485 N/m. The polished and fractured surfaces of specimens resulting from the mechanical tests were examined by scanning electron microscope (SEM) and energy dispersive X ray spectroscopy (EDS).

RESULTS AND DISCUSSIONS

Figure 2 depicts the DTG curves of the extruded cellulosic fibre-cement submitted to the supercritical CO_2 (SC) and noncarbonated (NC) curing respectively. According to the literature, the mass loss at 100 ºC is associated to the escape of the pore water, and the loss in the range between 100 ºC and 300 ºC is related to different stages of dehydration of the C-S-H (García-González et al., 2008). The major thermal decomposition

for cellulose occurs within a narrow temperature region ranging from 300 to 380 °C. Mass loss corresponding with the peak of 450 °C shown in the DTG curve is reported as the dehydroxylation of the $Ca(OH)_2$ and the peak of 700 °C is related to the decarbonation of $CaCO_3$. The non-carbonated composite presented higher mass loss in the peak of 450 °C of, approximatelly, 1.6%, than the carbonated counterpart around 1.3% for specimens after curing. For the peak at 700 °C, noncarbonated composites presented approximatelly 18.8%, but the supercritical carbonated composites showed higher mass loss around 23.2%, suggesting higher $CaCO_3$ content in the matrix as a result of the carbonation reactions.
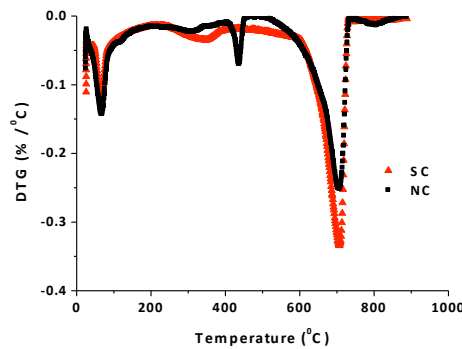
Figure 2 - DTG curves of the extruded cellulosic fibre-cement submitted to supercritical CO₂ (SC) and non-carbonation (NC) curing treatments.

According to literature, another effect of carbonation concerns the reduction of Ca/Si of calcium silicate hydrate gel, as well as that of other solid phases containing Ca^{2+}, which means that not only portlandite is carbonated and contributes to calcite formation (Short et al., 2001; García-González et al., 2008; Fabbri et al., 2009). Figure 3 shows that the massive precipitation of calcium carbonate after supercritical carbonation in the initial age leads to decreased water absorption and increasing bulk density. Both phenomena can be explained by the pore filling action of the carbonation, which most probably also leads to a pore refinement of the microstructure. The decrease of the water absorption and the increase of the bulk density indicate that both mass and volume of the precipitated hydration and carbonated products were higher than the one dissolved and/or leached during 200 cycles of accelerated ageing of soak and dry (200c) for both non-carbonated (NC) and carbonated (SC) composites.
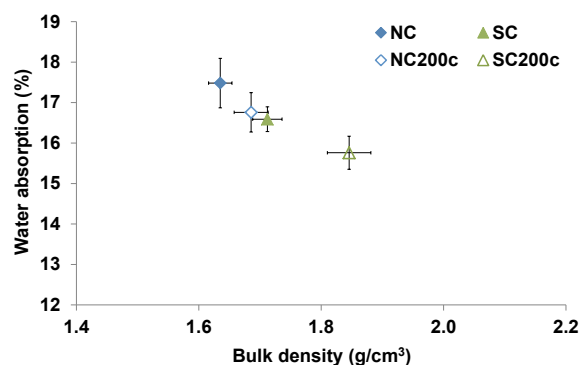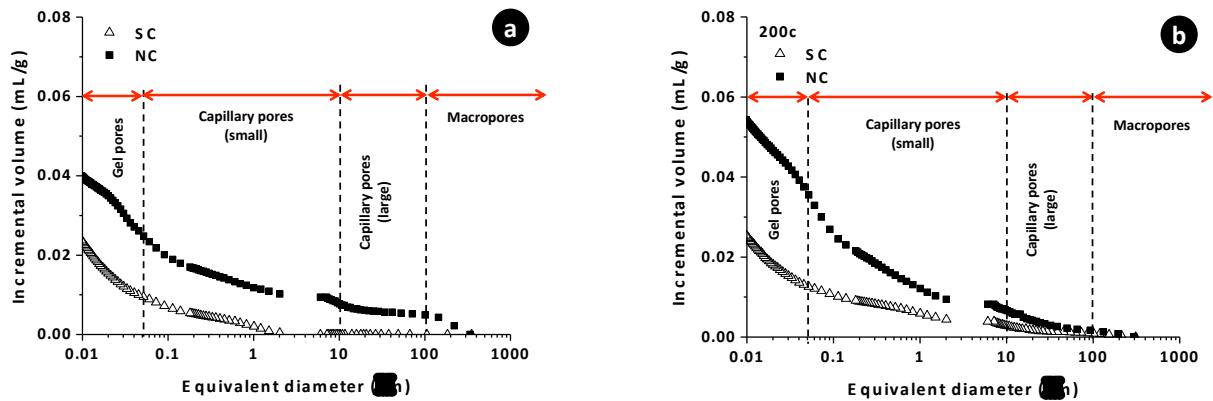

Figure 3 - Correlation between water absorption and bulk density of extruded cellulosic fibre-cement submitted to supercritical CO₂ (SC) respectively non-carbonation (NC) curing treatment, before and after exposure to 200 soak and dry cycles (200c).

The microstructure fibre-cement exhibits the presence of different pore scales and types, which are the result of the actual water/cement ratio, hydration cement kinetics, characteristics of the fibres and production process. According to Tian et al. (2011), pore structure of fibre-cement can be divided into bulky pore or macroporosity (100 μm~1 mm), capillary pores (0.05 μm~ 100 μm) and hydrated phases gel pores such as that of C-S-H (less than 50 nm).

Figure 4 depicts the changes in the incremental volume (mercury intruded/pore volume) and pore size (equivalent diameter) curves of non-carbonated extruded cellulosic fibre-cement compared to that of the fibre-cement products carbonated with the supercritical CO_2. It was noted that the non-carbonated composite has higher amount of capillary and gel pores than the carbonated composite before and after accelerated ageing (200c). A major reason for the pore complexity of cement based materials is that the main reaction product, C-S-H forms with a significant volume fraction of internal, nanometres-scale pores (Jennings et al., 2008). Moreover, it is known that pores and non-uniform cross-sections of cellulose fibres also promote capillary pores in the fibre/matrix interfacial zones. Figure 5 shows the SEM micrographs in back-scattered mode of the non-carbonated (Figure 5a) and carbonated (Figure 5b) composites. The SEM micrograph (Figure 5b) indicates carbonated zones around the sisal fibre and eucalyptus pulp. The low viscosity and high density of the supercritical CO_2 allowed the massive precipitation of calcium carbonate during the accelerated carbonation causing decrease in the amount of capillaries and gel pores around fibres. The C-S-H + $CaCO_3$ phases were detected in the carbonated zones by energy dispersive X ray spectroscopy (EDS). Fabbri et al. (2009) found similar phases in cement paste without fibres that had been carbonated with supercritical CO_2.

Figure 4 - Pore size distribution with incremental volume (mercury intruded) curves of extruded cellulosic fibre-cement submitted to supercritical CO_2 (SC) respectively non-carbonation (NC) curing treatment: (a) before and (b) after exposure to 200 cycles of soaking and drying (200c).
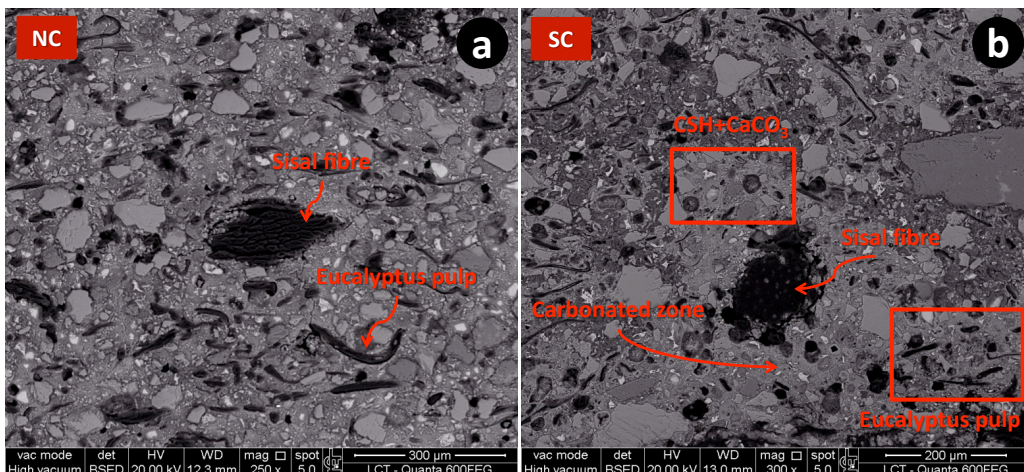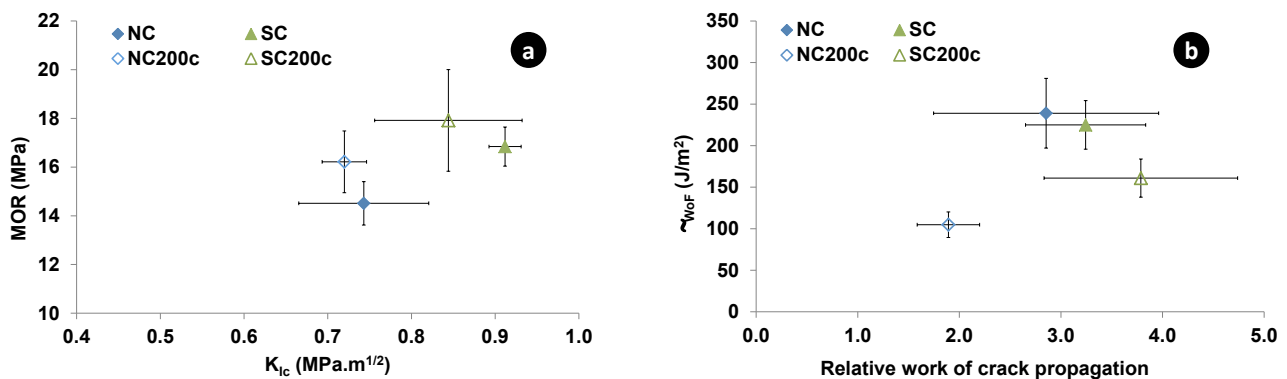

Figure 5 - SEM micrographs in the back-scattered mode (BSED) of extruded cellulosic fibre-cement submitted to (a) non-carbonation (NC) and (b) supercritical CO_2 (SC) curing treatment before accelerated ageing. The C-S-H + $CaCO_3$ phases were detected by energy dispersive X ray spectroscopy (EDS).

The early stage supercritical carbonation curing affected the mechanical behaviour of the fibre-cement as it can be observed in Figure 6. The average MOR-values showed a significant increase in the case of the

carbonated composite in the initial age (Figure 6a). Figure 6a illustrates that the supercritical carbonation curing was positive for the average K_{Ic}-values, resulting in more resistant materials to the crack propagation, if compared to non-carbonated fibre-cement. After accelerated ageing, the average MOR-values increased about 6%, but the average K_{Ic}-values have decreased for both composites. However, after exposure to 200 cycles of soaking and drying carbonated composites kept higher initial crack growth resistance (K_{Ic}) than non-carbonated, because of the microstructural refinement around the vegetable fibres.

The value of relative work of crack-propagation of the fibre-cement did not increase significantly after supercritical carbonation in the initial age (Figure 6b). However, after accelerated ageing the average value of relative work of crack propagation of the non-carbonated fibre-cement decrease 51%, but the carbonated composite maintained the average value of relative work of crack-propagation around 3.8. These results are associated essentially with two parameters: interfacial bond strength fibre/matrix and degradation of fibres in the cementitious matrix.

The fibre–matrix interactions are strongly dependent on physical and chemical adhesion, shear stress resistance and mechanical anchorage induced by deformations on the fibre surface and/or by overall complex geometry and orientation effects of the cellulosic fibres. The results that were obtained for the relative work of crack propagation (Figure 6b) indirectly show that there is an improvement in the fibre-matrix interface caused by supercritical carbonation in the curing stage, mainly after exposure to 200 soak and dry cycles. Besides, after accelerated ageing of 200 cycles the average values of energy of fracture (γ_{WoF}) of the carbonated and non-carbonated composite decrease approximately 28% and 56%, respectively. This indicates that a balanced physical-chemical adhesion between fibre and matrix was partially maintained by early stage supercritical carbonation after 200 soak and dry cycles. These results suggest that the toughening mechanisms in the fracture process of the carbonated composites, such as pull-out and bridging forces, were better preserved. This hypothesis is supported by the SEM-micrographs showed in Figure 7. Figure 7b illustrates that for the samples that were subjected to accelerated ageing, a higher amount of preserved sisal fibres is observed in the fracture surface of the supercritically carbonated fibre-cement when compared with the non-carbonated fibre-cement (Figure 7a).

Figure 6 - Correlation between (a) MOR versus fracture toughness, K_{Ic} and (b) energy of fracture, γ_{WoF}, and relative work of crack propagation of extruded cellulosic fibre-cement submitted to supercritical CO_2 (SC) respectively non-carbonation (NC) curing, before and after exposure to 200 cycles of soaking and drying (200c).
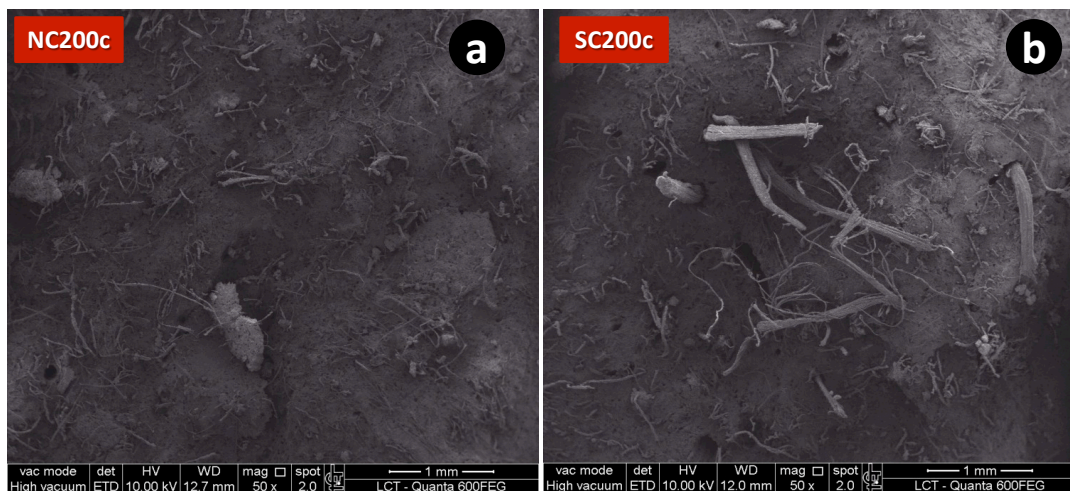
Figure 7 - SEM micrographs in the secondary electron mode of fracture surfaces of extruded cellulosic fibre-cement submitted to (a) non-carbonation (NC) and (b) supercritical CO_2 (SC) curing treatment, respectively, after exposure to 200 cycles of soaking and drying (200c).

These findings show the potential use of supercritical carbonation in the early stage of curing to improve the transition zone between the cellulosic fibre and the cementitious matrix. The results of this study show an interesting approach to mitigate degradation mechanisms of extruded cellulosic fibre-cement.

CONCLUSIONS

In the TGA, the carbonated composites showed higher mass loss related to $CaCO_3$ as expressed by the peak of 700 ^{o}C, approximately 23.2%, and lower mass loss related to $Ca(OH)_2$ as expressed by the peak of 450 ^{o}C, around 1.3%, as a result of the supercritical accelerated carbonation in the curing stage, if compared to non-carbonated composite.

The massive precipitation of calcium carbonate after accelerated carbonation in the curing stage, after pre-curing of three days, with supercritical CO_2 caused a refinement of the microstructure of the composite, thereby reducing water absorption and increasing bulk density. The mercury intrusion porosimetry measurements and SEM micrographs indicate that there is a large amount of calcium carbonate around the sisal fibre and eucalyptus pulp.

After accelerated ageing of 200 cycles of soaking and drying, the average values of energy of fracture ($\square_{WoF}$) of the carbonated and non-carbonated composites decrease approximately 28% and 56%, respectively.

The SEM micrograph of the carbonated fibre-cement fracture surface revealed that sisal fibres were better preserved after 200 soak and dry cycles due to the presence of carbonated zones.

ACKNOWLEDGEMENTS

REFERENCES

Almeida A E F S, Tonoli G H D, Santos S F, Savastano Jr H. 2010. "Effect of accelerated carbonation on kraft pulp fiber reinforced cement-based materials". *In* Proceedings: 1st TMS-ABM International Materials Congress, Rio de Janeiro, Brazil.

American Society for Testing and Materials - ASTM C150/C150M-11. 2011. "Standard Specification for Portland Cement".

American Society for Testing and Materials - ASTM C 948-81. 1981. "Test Method for Dry and Wet Bulk Density, Water Absorption, and Apparent Porosity of Thin Sections of Glass-Fiber Reinforced Concrete".

European Committee for Standardization, EN 494. 1994. "Fiber-cement profiled sheets and fittings for roofing – Products specification and test methods". BSI – British Standards Institution, London, UK.

Fabbri A, Corvisier J, Schubnel A, Brunet F, Goffé B, Rimmele G, Barlet-Gouédard V. 2009. "Effect of carbonation on the hydro-mechanical properties of Portland cements". Cement and Concrete Research 39 1156–1163.

García-González C A, Grouh Nadia el, Hidalgo Ana, Fraile Julio, López-Periago, Andrade Ana M., Carmen, Domingo Concepción. 2008. "New insights on the use of supercritical carbon dioxide for the accelerated carbonation of cement pastes". Journal of Supercritical Fluids 43 500–509.

Ginneken Luc Van, Dutré V, Adriansens W, Weyten H. 2004. "Effect of liquid and supercritical carbon dioxide treatments on the leaching performance of a cement-stabilised waste form". Journal of Supercritical Fluids 30 175–188.

Jennings H M , Bullard J W , Thomas J J, Andrade J E , Chen J J, Scherer G W. 2008. "Characterization and Modeling of Pores and Surfaces in Cement Paste: Correlations to Processing and Properties," Journal of Advanced Concrete Technology 6 (4) 5–29.

Kajita Y, Kariya S, Kozuka H, Holanda T, Ota S. 1997. "Development a method for quantitative assessment of flexibility and its application for evaluating MgO–CaO–ZrO2 bricks". *In* Proceedings of Unified International Technical Conference on Refractories – UNITECR, p. 337–34.

Martinez-Correa H A, Magalhães P M, Queiroga C L, Peixoto C A, Oliveira A L, Cabral F A. 2011. "Extracts from pitanga (Eugenia uniflora L.) leaves: Influence of extraction process on antioxidant properties and yield of phenolic compounds". Journal of Supercritical Fluids 55 998–1006.

Mohr B J, Biernacki J J, Kurtis K E. 2007. Supplementary cementitious materials for mitigating degradation of kraft pulp fiber-cement composites. Cement and Concrete Research 37 1531–1543.

Morton J H, Akers S A S, Cooke T. 2006. "Performance of slash pine fibers in fiber cement products". *In* Proceedings: 10th International Inorganic Bonded Composite Materials Conference IIBCC, São Paulo – Brazil, p.168-177.

Nakayama J. "Direct measurement of fracture energies of brittle heterogeneous materials". 1965. Jornal American Ceramic Society. 48 583-587.

Peter M A, Muntean A, Meier S A, Böhm M. 2008. "Competition of several carbonation reactions in concrete: A parametric study". Cement and Concrete Research 38 1385–1393.

Ribeiro S, Rodrigues J A, 2010. "The influence of microstructure on the maximum load and fracture energy of refractory castables". Ceramics International 36 263-274.

Sakai M, Bradt RC, 1993. "Fracture toughness testing of brittle materials". International Materials Reviews 38 53-78.

Shao Y, Wan S, He Z. 2011. "Manufacturing of cellulose fiber reinforced cement composites using carbon dioxide curing". *In* Proceedings: 16th International Conference on Composite Structures - ICCS, Porto, Portugal.

Soroushian P, Won J-P, Hassan M. 2012. "Durability characteristics of CO_2-cured cellulose fiber reinforced cement composites". Construction and Building Materials 34 44–53.

Short N R, Purnell P, Page C L. 2001. Preliminary investigations into the supercritical carbonation of cement pastes. Journal of Materials Science 36 35–41.

Tian L, Zhang Yu-e, Li F-m, Zhang H-y. 2011. "Research on Fine Structure of Strain Hardening Cement-based Composites (SHCC) by Inside Saline Waterproof". Applied Mechanics and Materials 71-78 1209-1212.

Tolêdo Filho R D, Ghavami K, England G L, Scrivener K. 2003. "Development of vegetable fibre–mortar composites of improved durability". Cement and Concrete Composites 25 185–196.

Tonoli G H D, Rodrigues Filho U P, Savastano Jr H, Bras J, Belgacem M N, Rocco Lahr F A. 2009. "Cellulose modified fibres in cement based composites". Composites: Part A 40 2046–2053.